A REVIEW OF STRUT-AND-TIE MODELS FOR FRP REINFORCED DEEP BEAMS

Taylor J. Brodbeck, Giorgio T. Proestos, and Rudolf Seracino

March 24th, 2024

NC STATE UNIVERSITY

THE WORLD'S GATHERING PLACE FOR ADVANCING CONCRETE

aci CONCRETE CONVENTION

Introduction

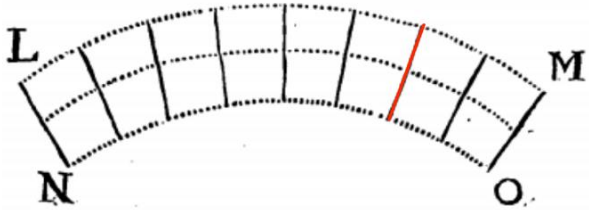

Robert Hooke's beam
(1678)

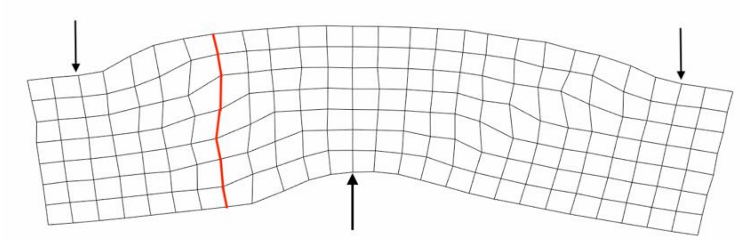

Experimental Data of a Deep Beam
(x10 magnification)

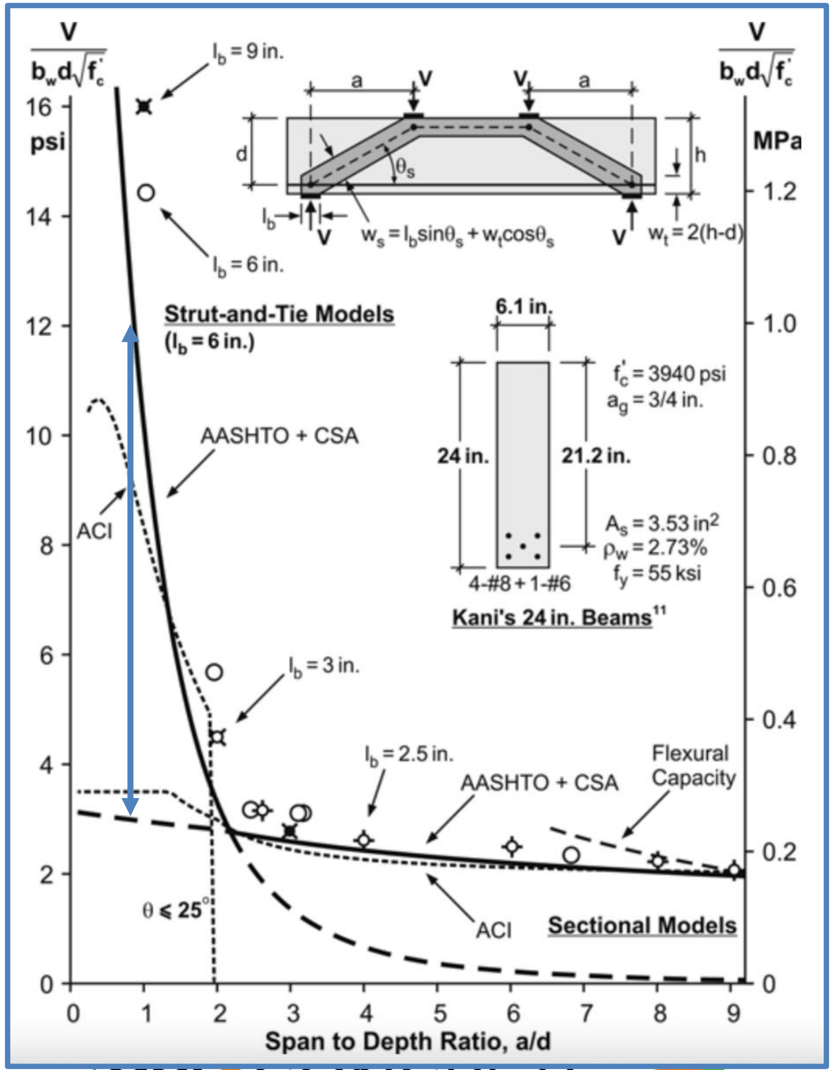

Strut-and-Tie Models

Strut-and-tie stress limits are empirical and based on tests of deep beams reinforced with steel bars.

Little experimental data exists for deep beams reinforced with only FRP bars, and results are variable.

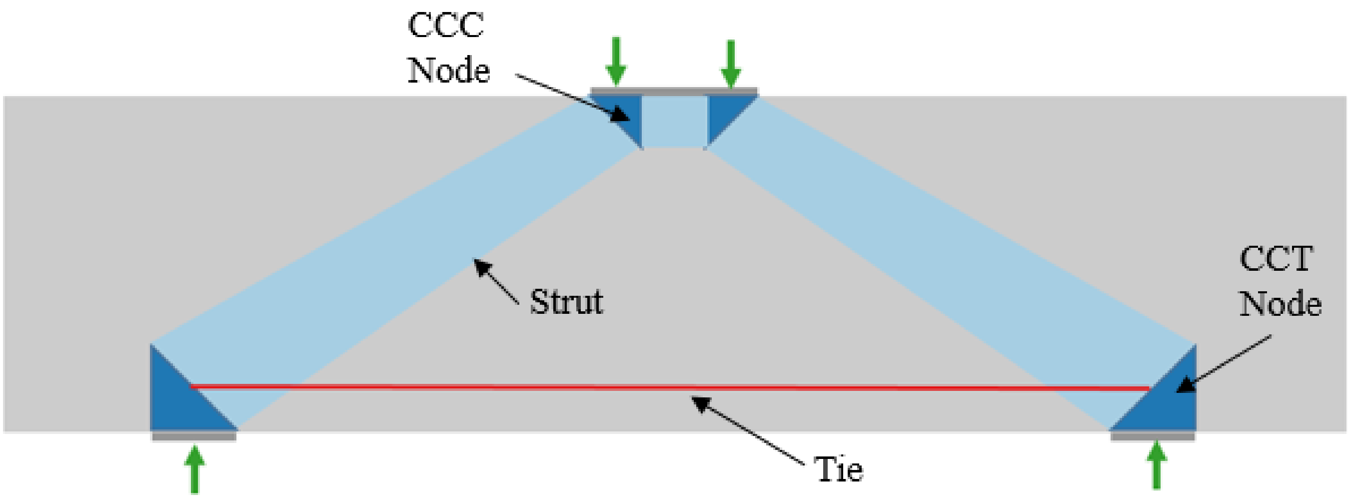

ACI Strut Reduction Factors

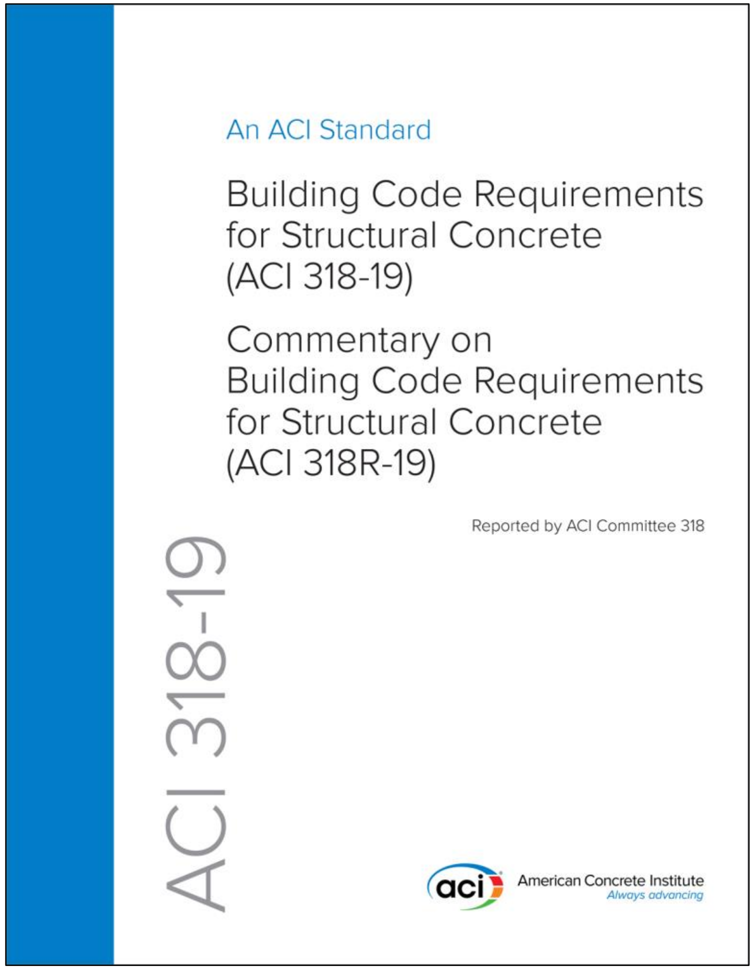

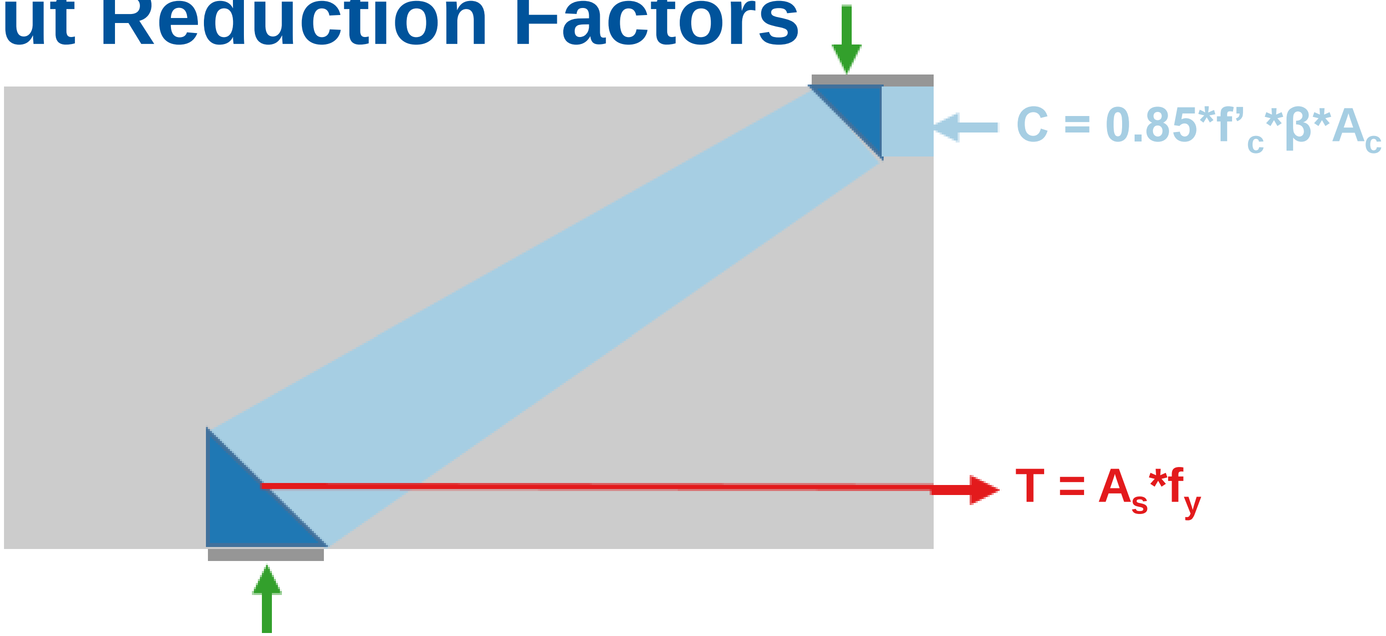

- β is an empirical reduction factor determined from experimental results of steel reinforced disturbed regions.
- For struts in a tension zone, β = 0.4
- Nodal reduction factors are a function of how many ties form into a node.

ACI 440

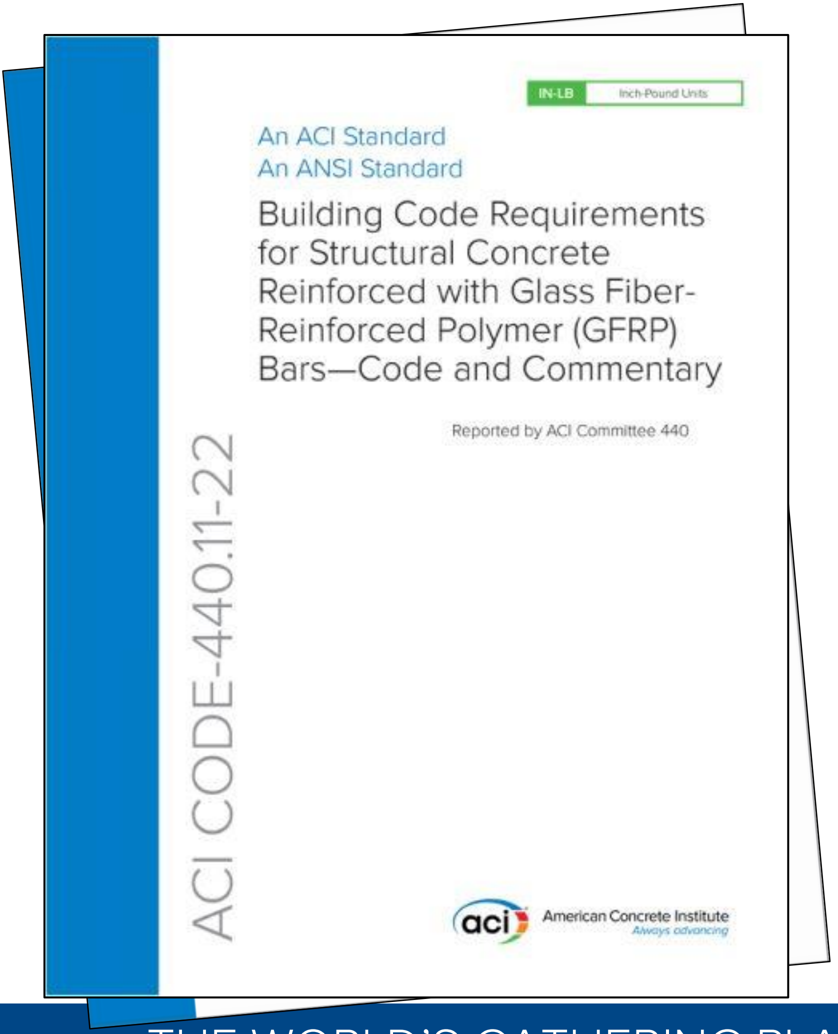

"CHAPTER 23 – STRUT-AND-TIE METHOD – NOT ADDRESSED"

ACI TAC in their Winter 2022 review of ACI440.11: *"This seems to be a large gap in 440 Code provisions that a designer may not appreciate. Preferred solution is to add a strut-and-tie modeling section."*

CSA Strut Reduction Factors

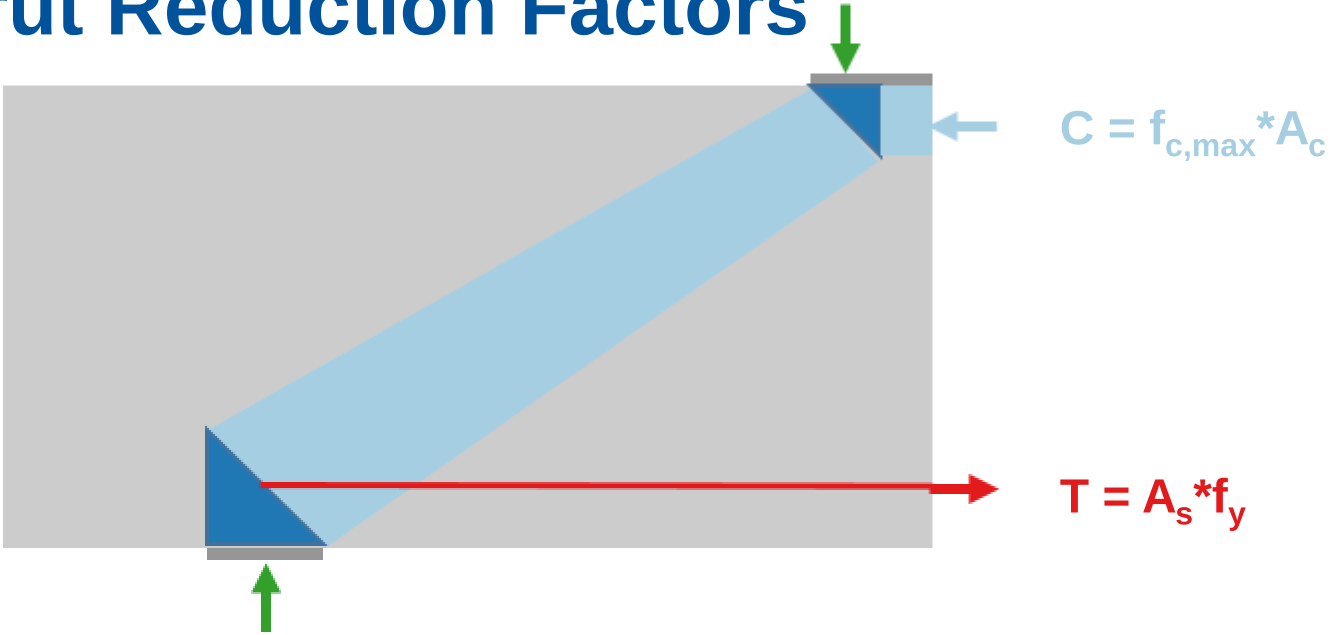

The strain in the tie softens the response of the concrete in compression.

$$\text{“}\beta\text{”} = \frac{1}{0.8+170\varepsilon_1} \leq 0.85$$

$$\varepsilon_1 = \varepsilon_S + (\varepsilon_S + 0.002)cot^2\theta_s$$

CSA Strut Reduction Factors

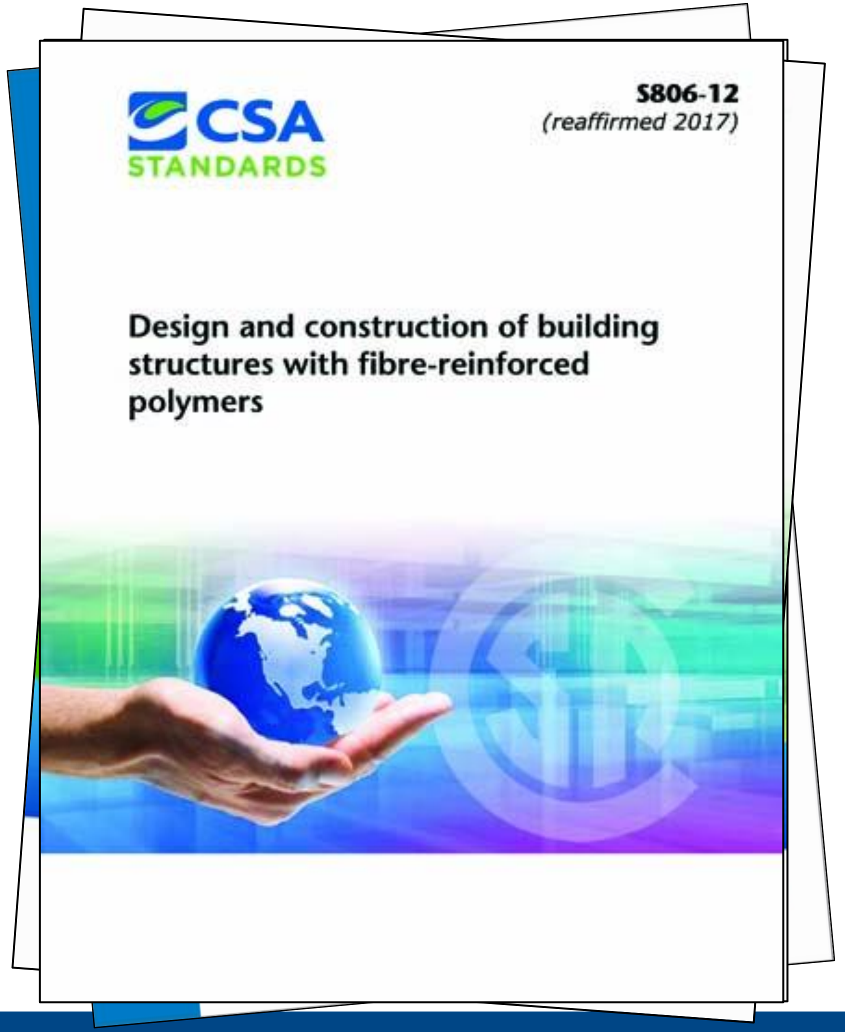

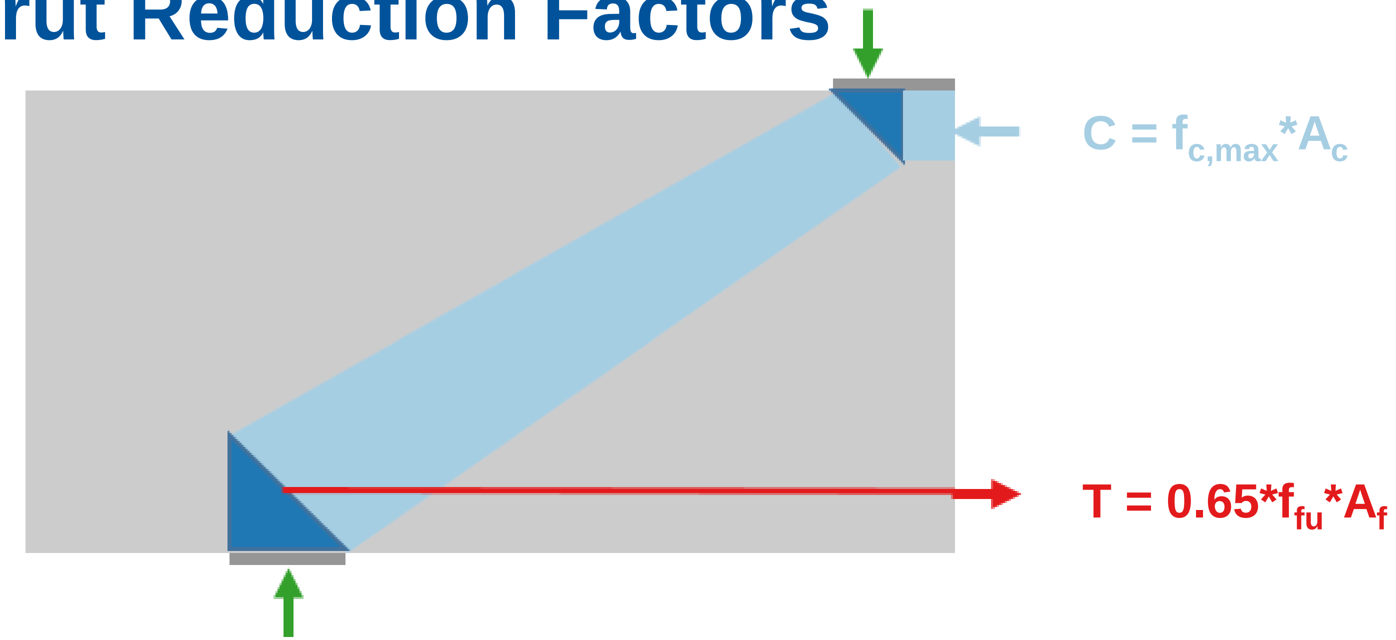

The strain in the tie softens the response of the concrete in compression.

$$\text{"}\beta\text{"} = \frac{1}{0.8+170\varepsilon_1} \leq 0.85$$

$$\varepsilon_1 = \varepsilon_F + (\varepsilon_F + 0.002)cot^2\theta_s$$

Published Tests

Authors	Beam	a/d	Longitudinal Reinforcement Type	Longitudinal Reinforcement Ratio (%)	Shear Reinforcement Type	Shear Reinforcement Ratio (%)
Andermatt and Lubell (2013)	A1N	1.07	Glass	1.49	-	-
	A2N	1.44	Glass	1.47	-	-
	A3N	2.02	Glass	1.47	-	-
	A4H	2.02	Glass	1.47	-	-
	B1N	1.08	Glass	1.70	-	-
	B2N	1.48	Glass	1.71	-	-
	B3N	2.07	Glass	1.71	-	-
	B4N	1.48	Glass	2.13	-	-
	B5H	1.48	Glass	2.12	-	-
	B6H	2.06	Glass	1.70	-	-
	C1N	1.10	Glass	1.58	-	-
	C2N	1.49	Glass	1.56	-	-
Farghaly and Benmokrane (2013)	G8N6	1.14	Glass	0.69	-	-
	G8N8	1.15	Glass	1.24	-	-
	C12N3	1.13	Carbon	0.26	-	-
	C12N4	1.13	Carbon	0.46	-	-

Published Tests

Authors	Beam	a/d	Longitudinal Reinforcement Type	Longitudinal Reinforcement Ratio (%)	Shear Reinforcement Type	Shear Reinforcement Ratio (%)
Mohamed et al. (2017)	G1.47	1.47	Glass	1.24	-	-
	G1.47H	1.47	Glass	1.24	Horizontal, Glass	0.68
	G.147V	1.47	Glass	1.24	Vertical, Glass	0.42
	G1.13	1.13	Glass	1.24	-	-
	G1.13V	1.13	Glass	1.24	Vertical, Glass	0.42
	G1.13H	1.13	Glass	1.24	Horizontal, Glass	0.68
	G1.13VH	1.13	Glass	1.24	Vertical and Horizontal, Glass	0.42(V) and 0.68(H)
	G0.83	0.83	Glass	1.24	-	-
	G0.83H	0.83	Glass	1.24	Horizontal, Glass	0.68
	G0.83V	0.83	Glass	1.24	Vertical, Glass	0.42
Krall and Polak (2019)	BM12-INF	2.50	Glass	2.51	-	-
	BM16-INF	2.50	Glass	2.23	-	-
	BM25-INF	2.50	Glass	1.82	-	-
	BM12-220	2.50	Glass	2.51	Glass	0.51
	BM16-220	2.50	Glass	2.23	Glass	0.51
	BM25-220	2.50	Glass	1.82	Glass	0.51
	BM12-150	2.50	Glass	2.51	Glass	0.75
	BM16-150	2.50	Glass	2.23	Glass	0.75
	BM25-150	2.50	Glass	1.82	Glass	0.75
	BM12-s230	2.50	Glass	2.18	Glass	1.19
	BM16-s230	2.50	Glass	1.94	Glass	1.19

Failure Modes: Diagonal Strut Crushing

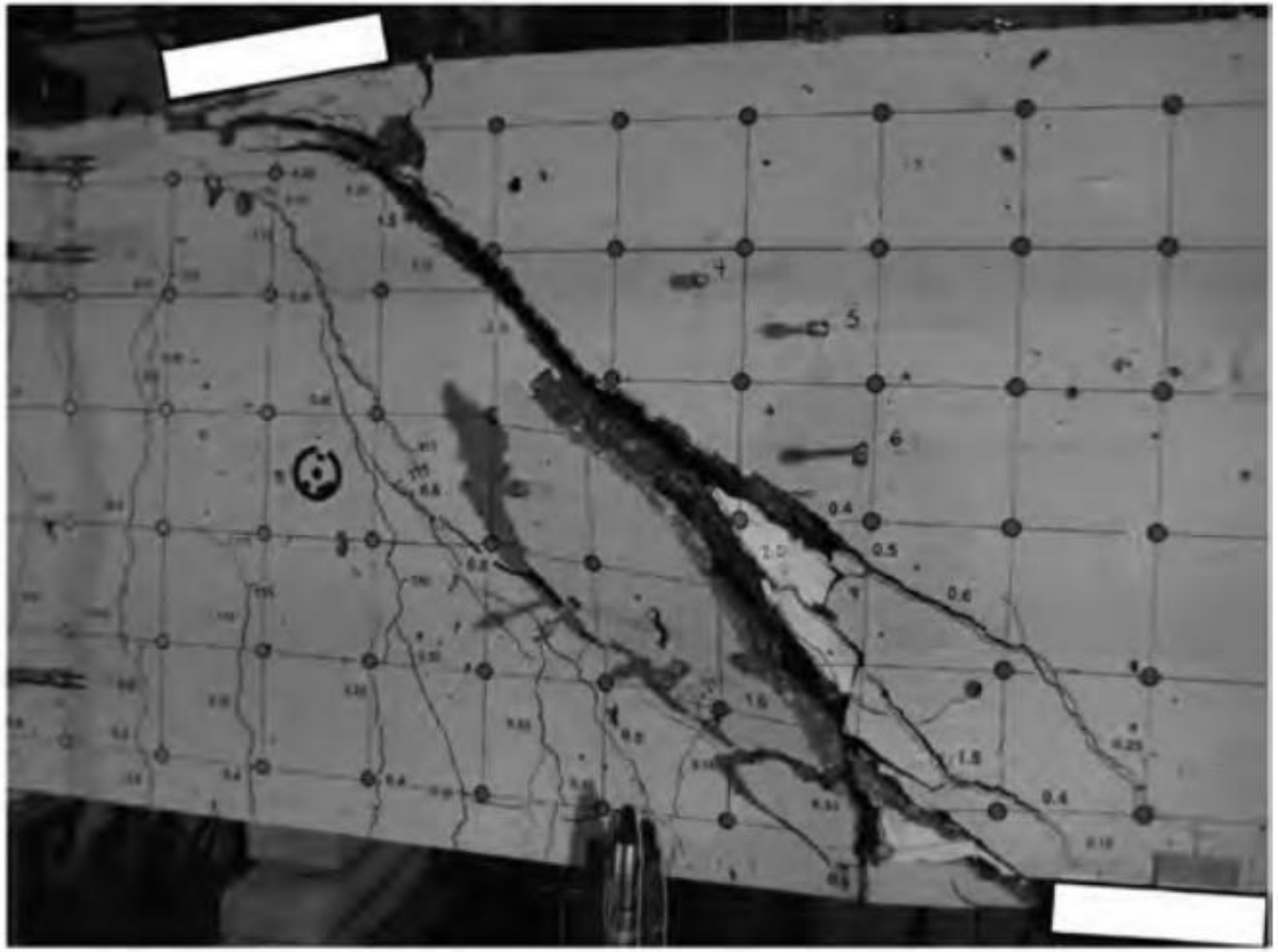

(Andermatt and Lubell, 2013)

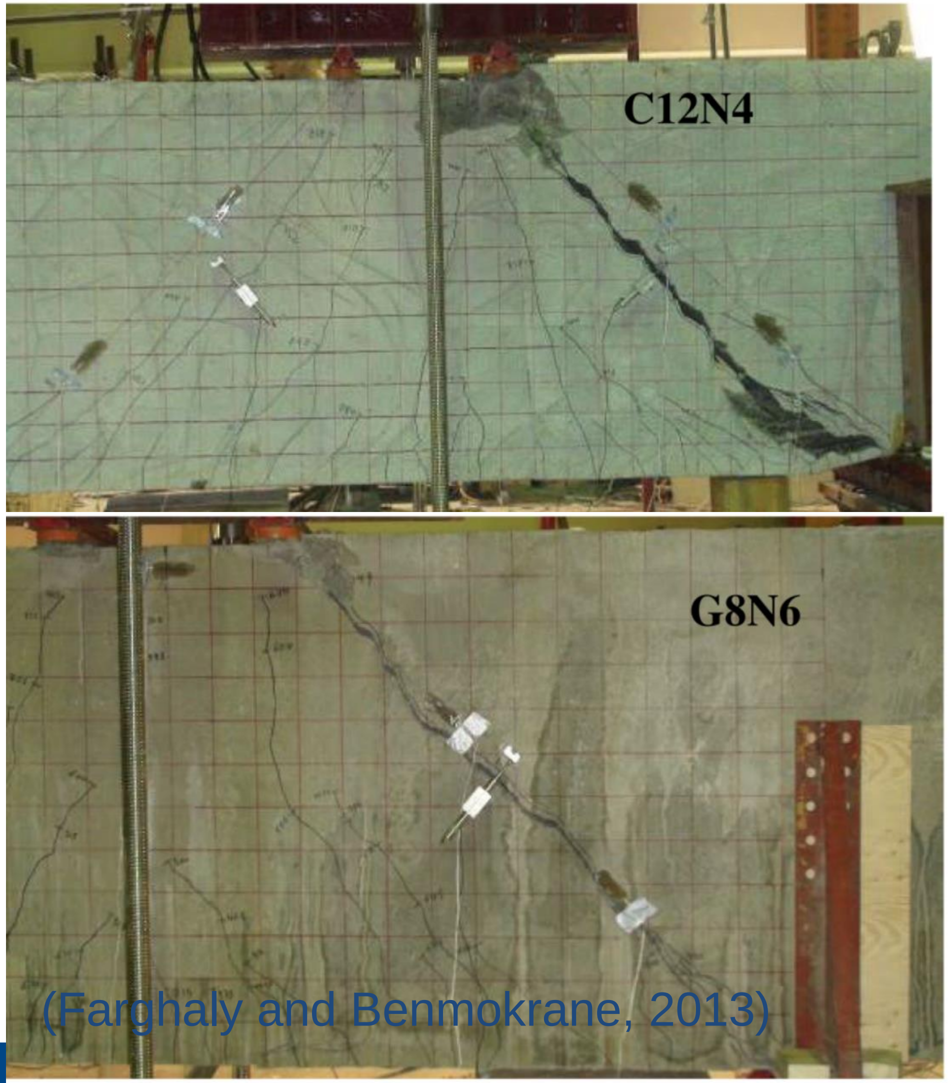

(Farghaly and Benmokrane, 2013)

Failure Modes: Flexural Compression

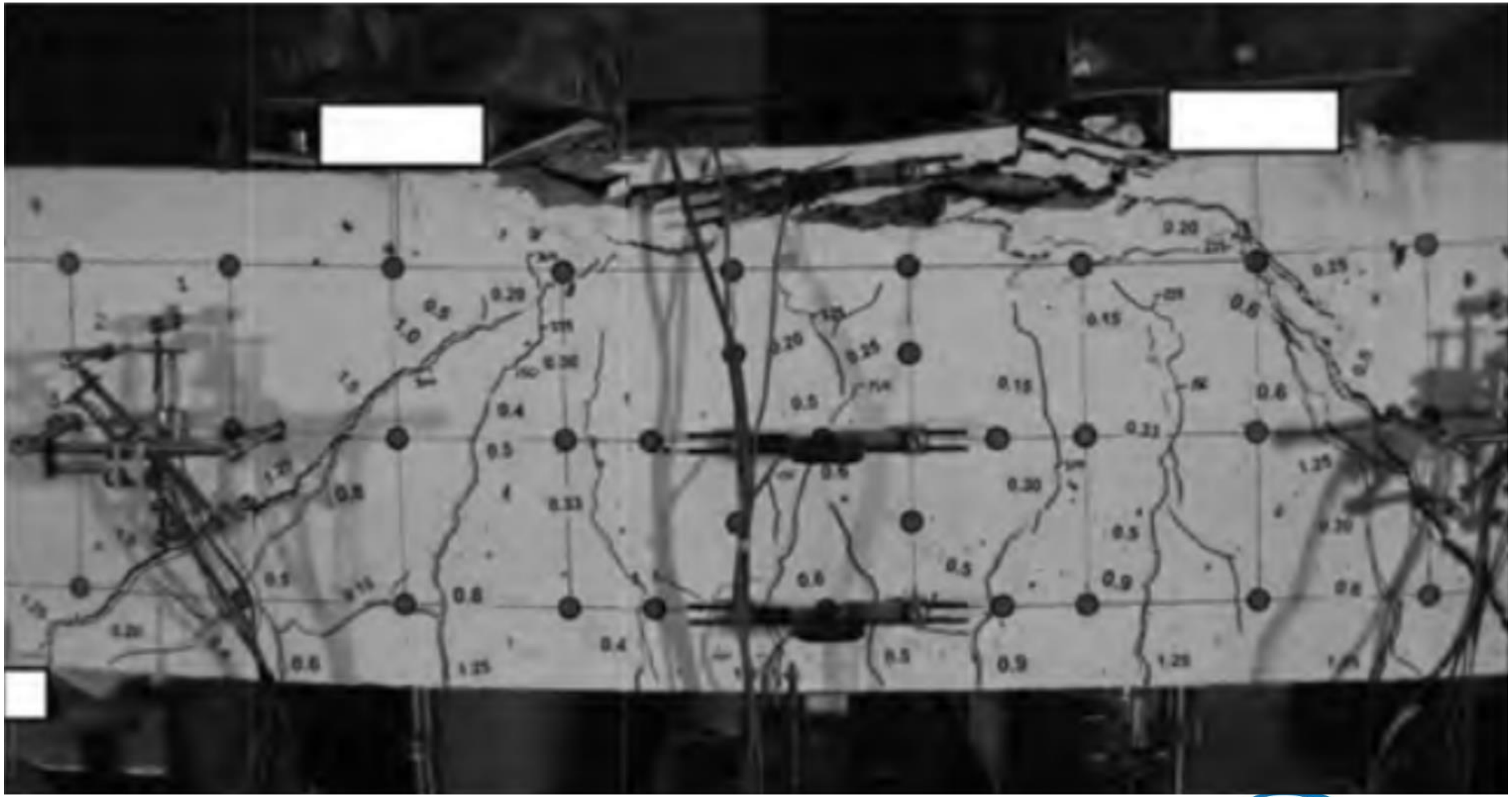

(Andermatt and Lubell, 2013)

Failure Modes: Shear Compression

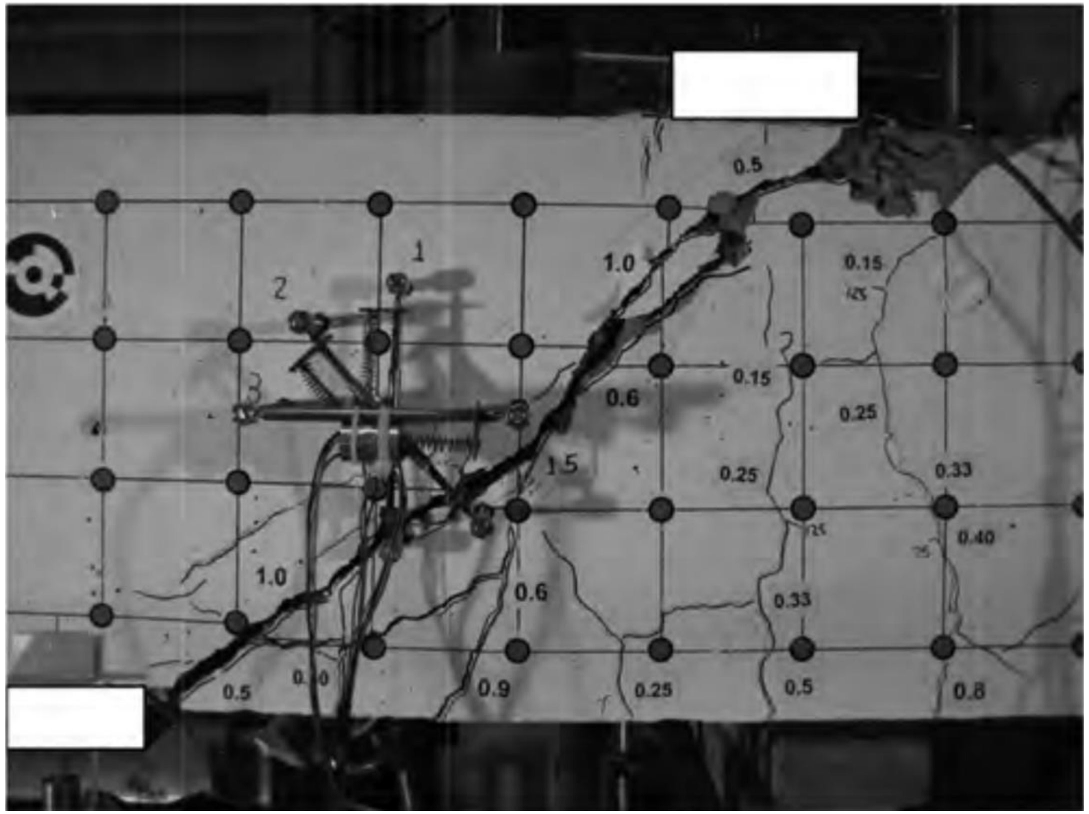

(Andermatt and Lubell, 2013)

A failure mode unique to FRP beams occurred in these tests in 4-point bending by *Andermatt and Lubell (2013)* wherein the presence of the shear crack limited the depth of the concrete compression zone.

Effect of height on shear capacity

Especially at smaller a/d ratios, the impact of specimen height on shear capacity is evident and necessitates large-scale testing

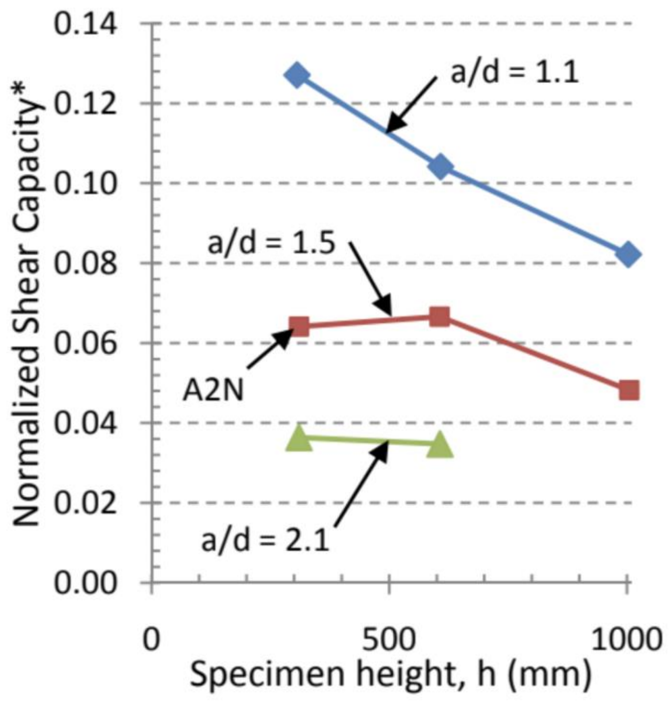

(Andermatt and Lubell, 2013)

Glass vs. Carbon FRP

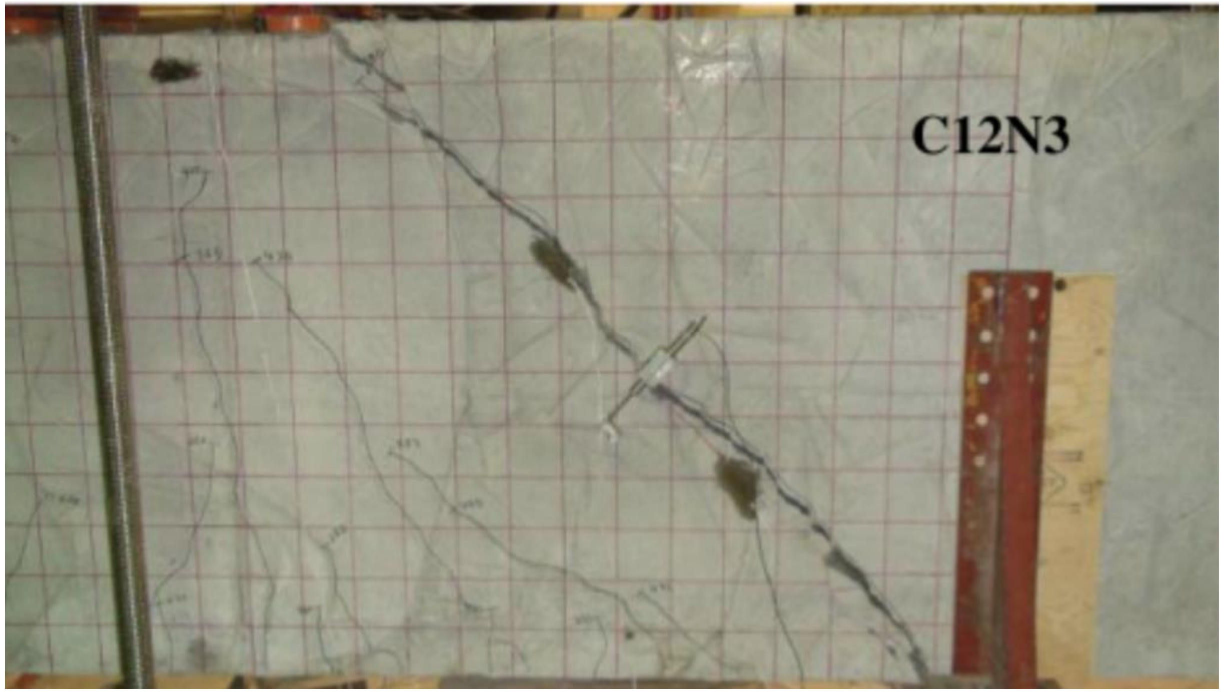

(Farghaly and Benmokrane, 2013)

Tests by Farghaly and Benmokrane (2013) compared the behavior of Glass and Carbon FRP.

For beams with similar axial stiffnesses (E_fAf), the capacity was similar.

Glass vs. Carbon FRP

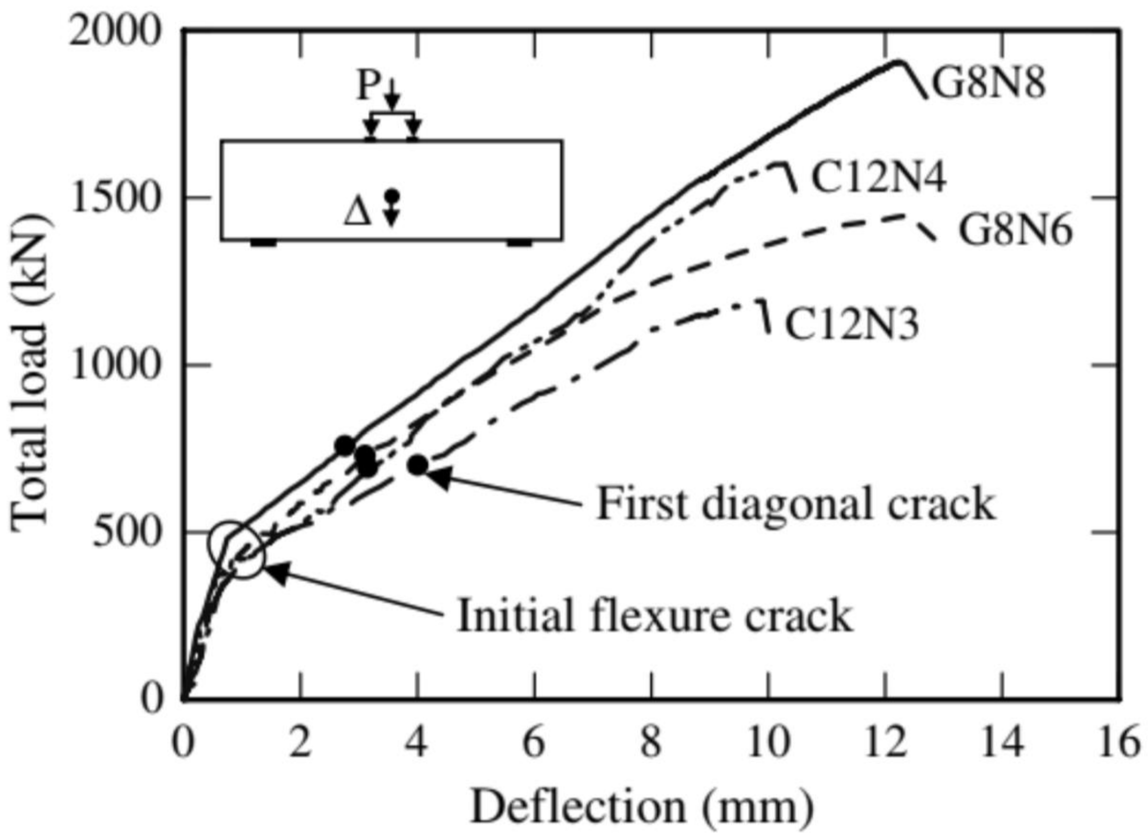

(Farghaly and Benmokrane, 2013)

Differences in capacities between G8N8 and C12N4, and G8N6 and C12N3, can be attributed to differences in f_c

Influence of Shear Reinforcement

The use of stirrups increased the extent of concrete crushing.

Horizontal shear reinforcement decreased capacity while vertical shear reinforcement increased capacity.

(a) (b) (c)

(Mohamed et al., 2017)

Influence of Shear Reinforcement

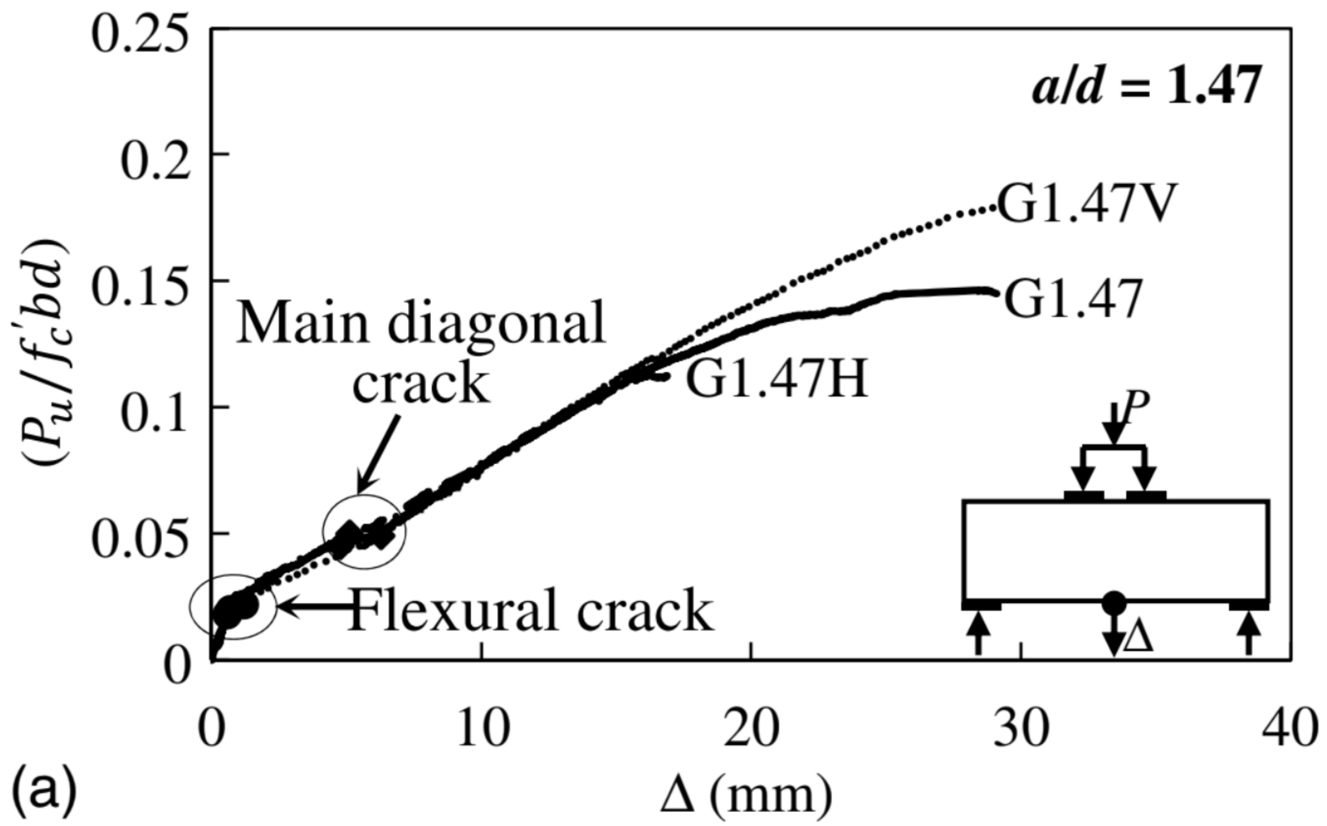

(Mohamed et al., 2017)

Horizontal shear reinforcement reduced capacity by increasing tension in the concrete strut

Vertical shear reinforcement increased the capacity

Comparison with ACI 318

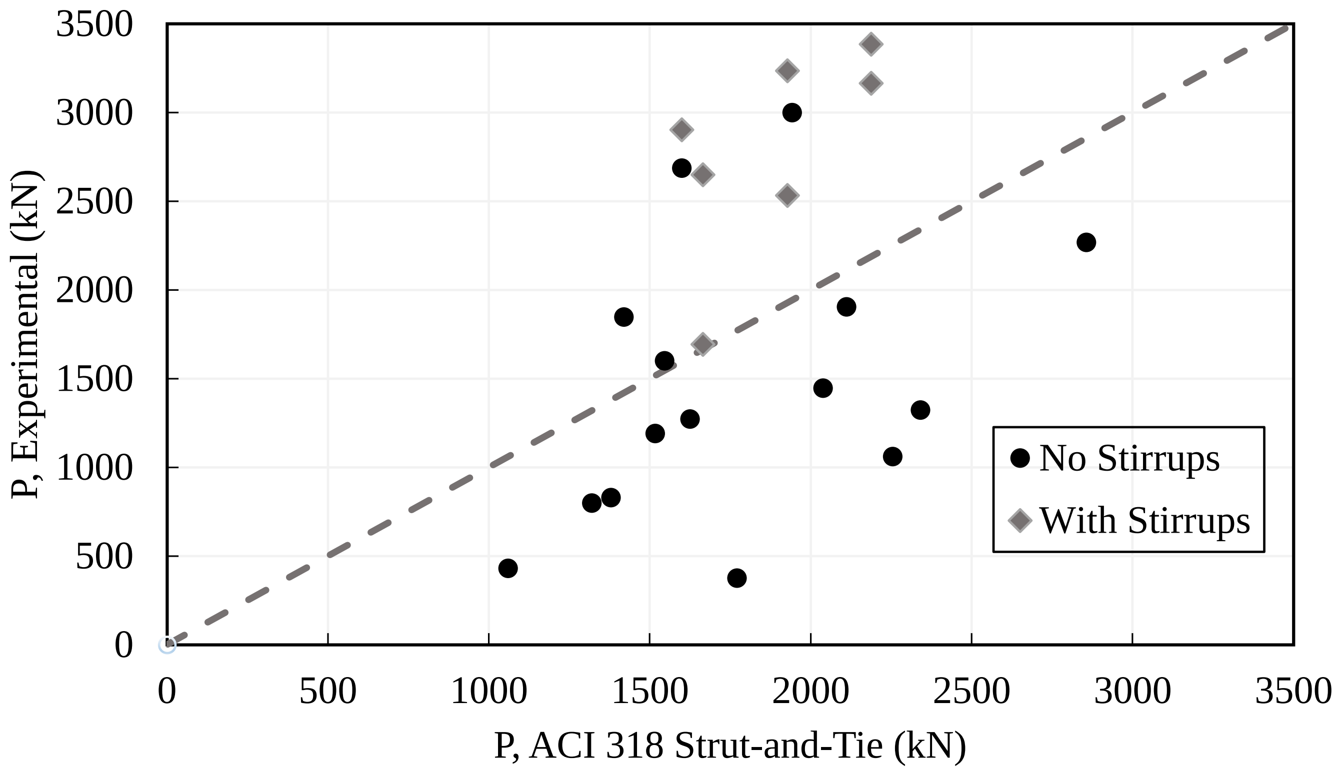

Using the strut and nodal factors from ACI 318 (developed for steel reinforced deep beams), the calculated capacity is unconservative compared to experiments.

Comparison with CSA S806

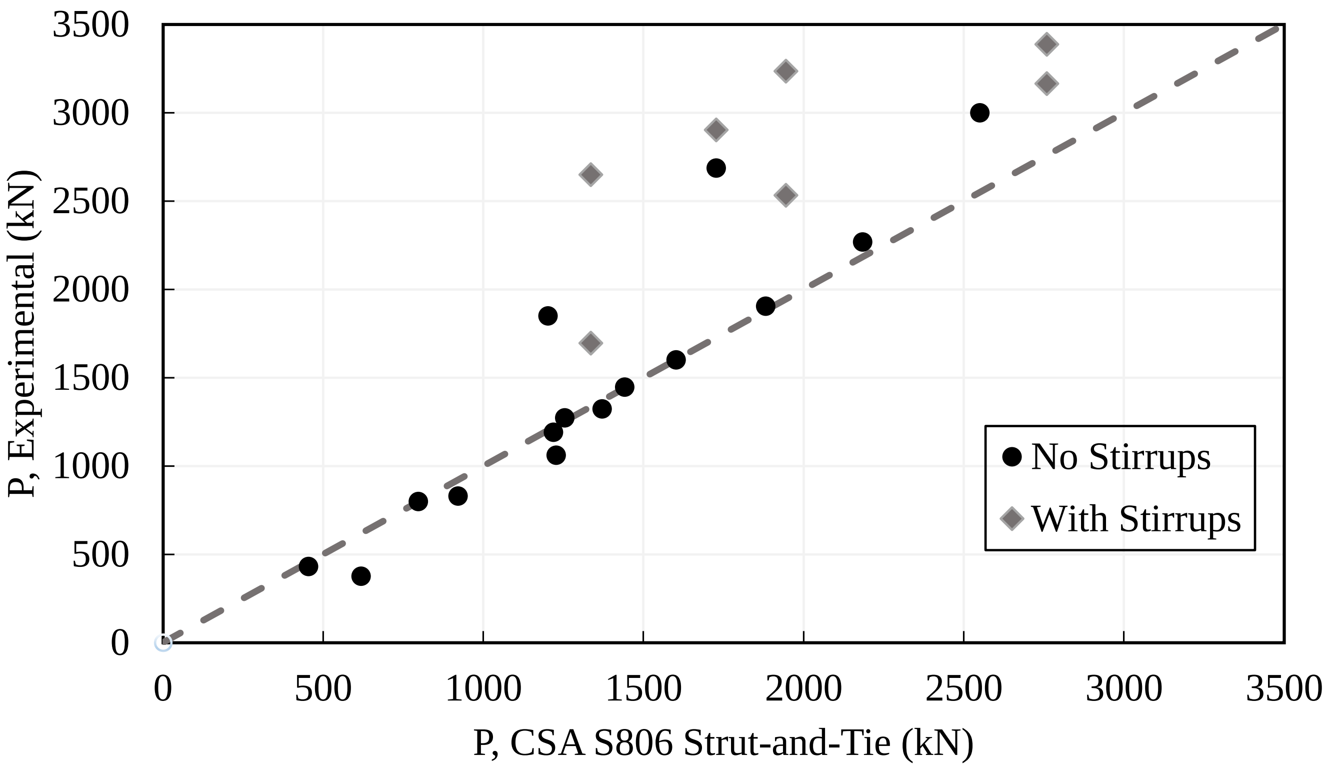

The CSA S806 strut-and-tie strut reduction factors are the same as CSA A23. Using the strain in the reinforcement to predict the softening of the surrounding concrete resulted in more accurate estimates of capacity.

Indeterminate Strut-and-Tie Model

This strut-and-tie model incorporates the shear reinforcement as vertical ties, uses the modified compression field theory to estimate concrete capacity.

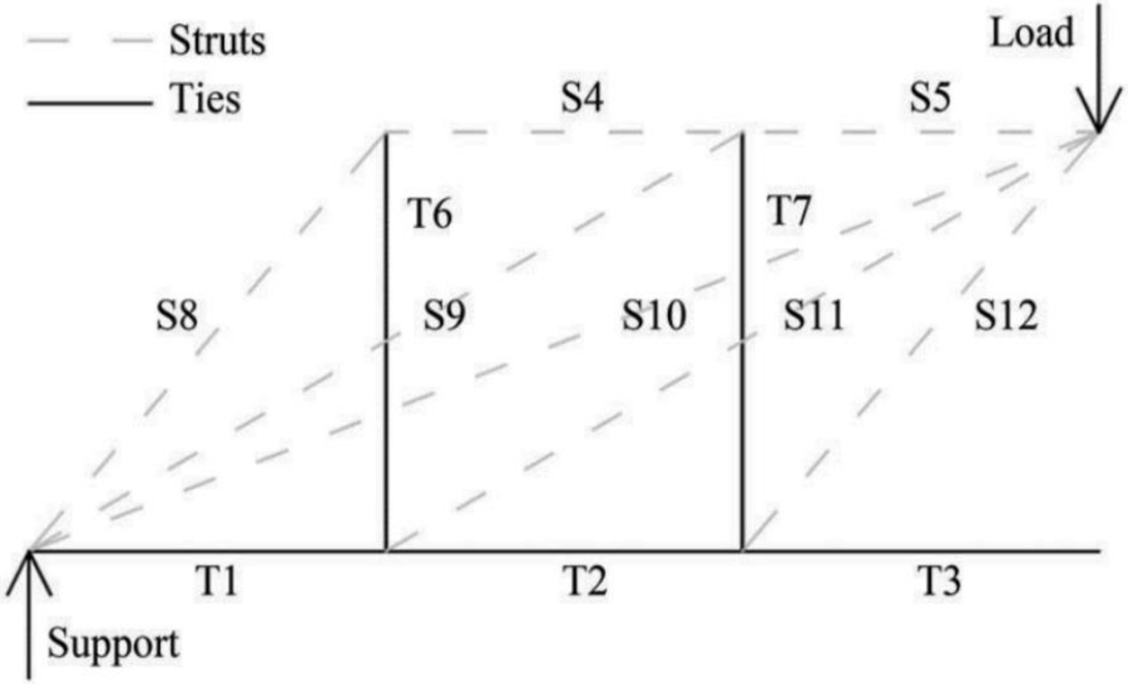

(Liu and Polak, 2022)

Cracked Strut-and-Tie Model

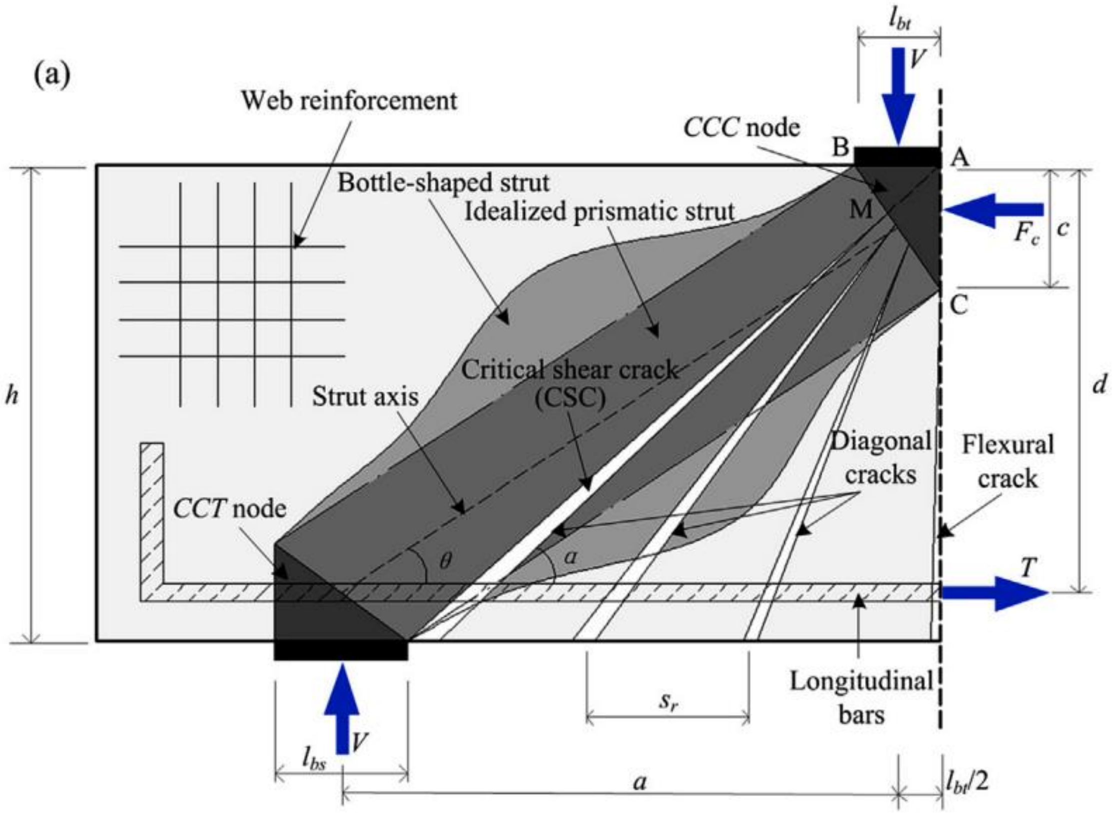

(Chen et al., 2020)

Similar to compression softening, this model accounts for the tension in the concrete forming the compression strut.

Future Work: Shear Reinforcement

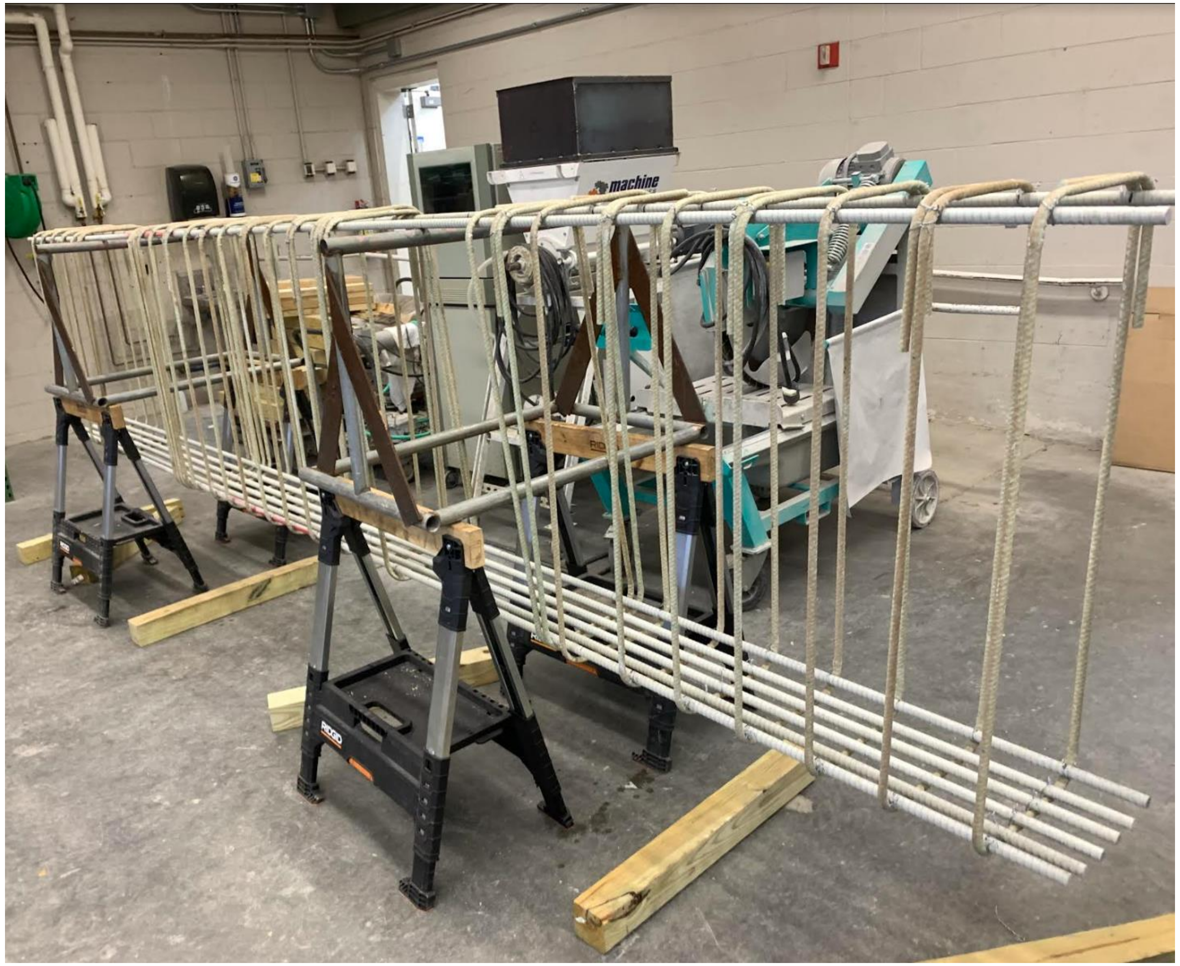

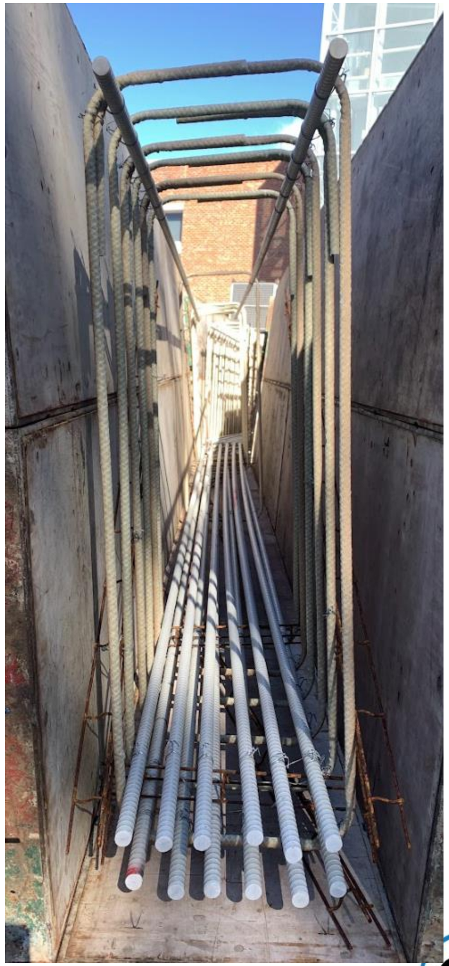

Future Work: Understanding Behavior with Full Field of View Instrumentation

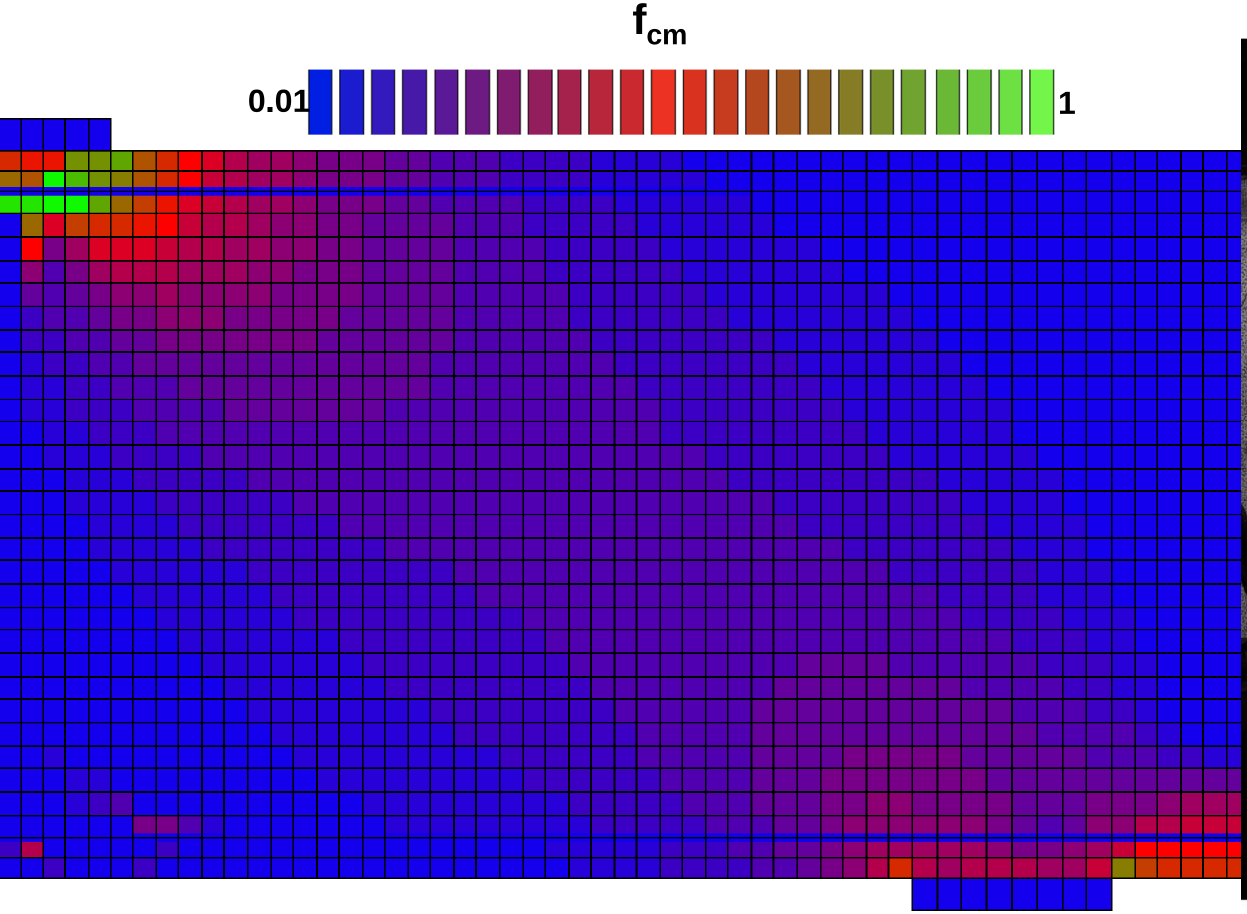

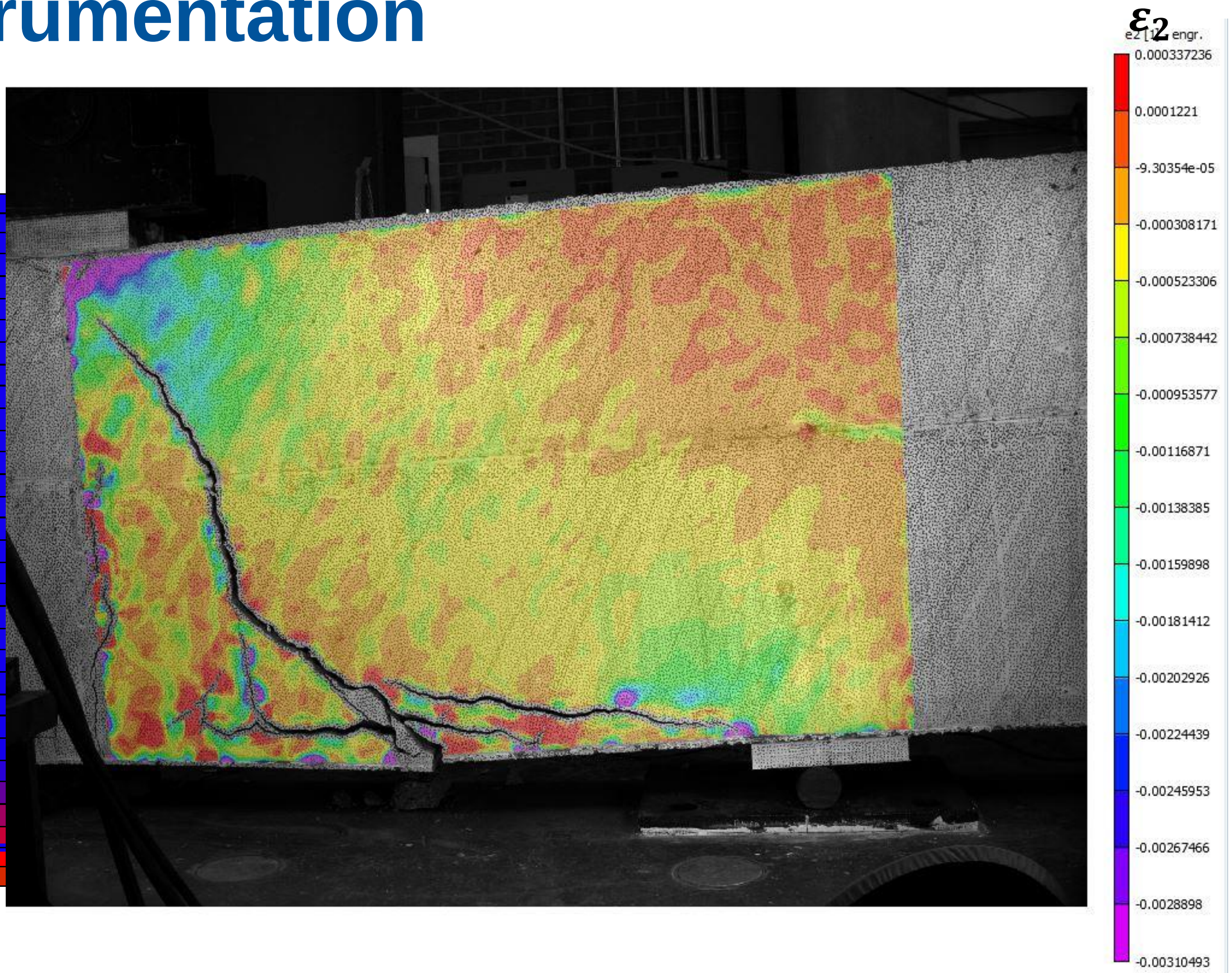

Thank You!

Questions?